Pergamon

Oral Oncol, Eur J Cancer Vol. 32B, No. 5, pp. 311-321, 1996

Printed in Great Britain
0964-1955/96 $15.00 + 0.00

PII: S0964-1955(96)00005-X

Papers

Imaging and Staging of Head and Neck Cancer Using a Low pH In-111–Bleomycin Complex

K.J.A. Kairemo,[1] H.A. Ramsay,[2] T. Paavonen[3] and S. Bondestam[4]

[1]Department of Clinical Chemistry; [2]Department of Otorhinolaryngology; [3]Department of Pathology; and [4]Diagnostic Radiology, Helsinki University, Haartmaninkatu 4, FIN-00290, Helsinki, Finland

Bleomycin (BLM), a natural antibiotic toxic to dividing cells has been used for treatment of several forms of cancer. BLM has been labelled with various cations but most have turned out to be unstable *in vivo*. In-BLM has demonstrated high bone marrow uptake, but by using an In-111–bleomycin complex (BLMC) formed at low pH, the low *in vivo* stability and high bone marrow uptake can be avoided. Our premise is to combine radiotherapy and chemotherapy by using radionuclide-BLMC.

In this study we used In-111–A'_{2a-c}–BLMC in 28 head and neck cancer patients. Scintigraphic findings were compared to those of surgery, pre-operative radiology and proliferation markers. The injected patient activity was approximately 85 MBq, 100 MBq/mg.

The half-life of In-111 activity in serum varied from 1.5 to 3.1 h, and in urine from 1.4 to 3.7 h. More than 95% of the urine activity was excreted within 24 h. From biopsies obtained from surgical specimens of 22 patients the absolute uptakes in tumour tissues varied between 0.10 and 0.95×10^{-3}% ID/g. Uptakes in normal tissues varied from 0.01 to 0.32×10^{-3}% ID/g, and were always lower than in malignant tissues of the same patients. All patients were examined on the injection day with ultrasonography of the neck. Using In-111–BLMC we missed small metastatic lymph nodes (<1 cm) in 2 patients, but there were no false positive findings. The critical organ from the dosimetric point of view was the kidney. The absorbed radiation doses with these injected activities were 19 mGy in liver, 75 mGy in kidney and 1.0 mGy in whole body (5 h mean residence time). Our results indicate that In-111–BLMC targets head and neck cancer, and identifies metastatic spread. It could possibly be applied with higher activities for adjuvant Auger-electron therapy of head and neck cancer.

Key words: bleomycin, head and neck neoplasms, indium radioisotopes, radionuclide imaging, tumour targeting

Oral Oncol, Eur J Cancer, Vol. 32B, No. 5, pp. 311–321, 1996

INTRODUCTION

Bleomycin (BLM) is a well-known natural antibiotic isolated from *Streptomyces verticillus* [1]. It is toxic to dividing cells and has been used for treatment of several forms of cancer since its discovery [2]. This polypeptide with a molecular weight of approximately 1400 D is a mixture of chromatographically different subgroups which differ from each other only by the terminal amine group. There are three different functional groups within the bleomycin structure: The galactose and mannose derivative, often considered to be responsible for recognising tumour cells, the metal chelating part, which activated this organometallic compound to act as an antitumour agent and the terminal part, which has a variable terminal amine thought to be responsible for DNA cleavage in tumour cells.

Bleomycin has been labelled with various mono (I)-, di (II)-, and trivalent (III) metal cations [3]; divalent cations copper, nickel, cobalt and zinc have demonstrated high affinity, whereas iron and mercury had low affinity. Alkaline earth metals and trivalent metals did not bind at all. A great number of metals have been tested, and many have failed either because of lacking *in vivo* stability or tumour affinity.

Correspondence to K.J.A. Kairemo.
Received 2 Nov. 1995; provisionally accepted 9 Jan. 1996; revised manuscript received 26 Jan. 1996.

EJC(B) 32:5-B

Clinically useful radiolabels are chromium-51 and cobalt-57. Nieweg *et al.* [4] presented a specificity of 98% in a Co-57–bleomycin staging study of 132 lung cancer patients. In another lung cancer staging study of 25 patients [5], only one false positive (a hamartoma), and three false negative findings were observed using Co-57–bleomycin. Recently, Co-57–bleomycin has proven to predict the response to chemotherapy in lung cancer patients [6].

Cobalt-57 is toxic and has an inconveniently long half-life (270 days). Therefore, other metals, such as Ga-67, Tc-99m and In-111 [7] have been introduced as radiolabels. They have all turned out to be unstable *in vivo*. Furthermore, In-111–bleomycin demonstrated high bone marrow uptake. However, Hou *et al.* [8] were able to show a higher uptake in glioma-bearing mice using In-111–bleomycin complex (BLMC) as compared to conventional bleomycin and its fractions. This BLMC did not demonstrate any affinity to transferrin, nor was there any bone marrow uptake. This complex was formed at low pH, had rapid kinetics and was stable *in vivo*. In a clinical study where In-111-A–bleomycin was used in 46 patients with orofacial neoplasms, a specificity of 100% and a sensitivity of 96% were observed [9]. In our preliminary study we used the fraction In-111-A'_{2a-c}–BLMC, which will be formed after labelling BLM at low pH 2.5 [10]. We found a sensitivity of 93% and specificity of 100% in 13 head and neck cancer patients [11].

The staging studies of head and neck cancer have been performed using other tracers, such as Tc-99m (V) dimercaptosuccinic acid [12], Co-57–bleomycin [13], gallium-67-citrate [14, 15], In-111–transferrin and P-32 [16]. Recently, monoclonal antibodies for clinical purposes have been introduced, such as antibodies against carcinoembryonic antigen [17, 18], squamous cell cancer (SCC)-cytokeratin associated antigen [19], epidermal growth factor receptor antigen [20], as well as the recently well characterised E48 and U36 SCC-specific monoclonal antibodies [21–23]. None of these antibodies has yet turned out to be a magic bullet in clinical tumour targeting studies.

The idea of combining radiotherapy and chemotherapy using a bleomycin complex is fascinating. Our intention is to develop a chemotherapeutic agent for cancer treatment, which is tumour seeking and can be linked to an Auger-emitter. This is the report of our study using In-111-A'_{2a-c}–BLMC in different stages of head and neck cancer. Scintigraphic findings after using a diagnostic dose of In-111–BLMC were compared with those of surgery, pre-operative radiology (including transoesophageal ultrasound in some cases) and mitotic activity.

MATERIALS AND METHODS

In-111–*BLM complex*

In-111–BLMC was prepared by incubating 15 mg bleomycin as bleomycin sulphate (Lundbeck, Copenhagen, Denmark) dissolved in water with $^{111}InCl_3$ (Mallinckrodt, Petten, The Netherlands) at pH 2–2.5 for at least 30 min. This bleomycin sulphate consists of 13 alkaline glycopeptides. The compounds that formed In-111-complex were controlled by using thin layer chromatography [TLC, Silica plates, 85% MeOH; 15% NH_4Ac (10%-water solution)]. Figure 1 shows the chromatograms of BLM and BLMC, after incubating with In-111. The composition of radiolabelled BLM was studied in detail, first by TLC [Silica plates, 50% MeOH; 50% NH_4Ac (10%-water solution)], and then by separating different BLM fractions using gel chromatography (Sephadex C columns). Thin layer chromatography demonstrated three subgroups. Fractions A_1, B_1 and A'_{2a-c} were filtered through gel chromatography. This ion chromatographic column gave a partial separation between fractions A_1 and B_1, and a total separation to A'_2 subfractions a–c. These A'_{2a-c} subfractions formed In-111–BLMC. At low pH more than 95% of In-111 was coupled to subfraction A'_{2a-c}. Less than 10% of BLM contains this BLMC. More than 98% of In-111 was incorporated into In-111–BLMC. The injected patient

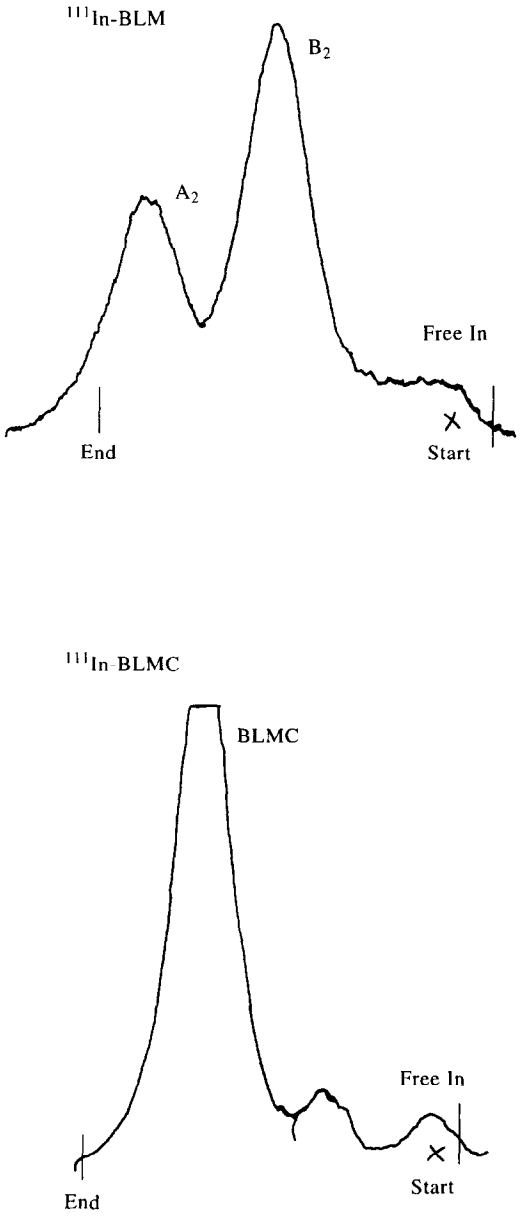

Fig. 1. A typical chromatogram of In-111–bleomycin complex (BLMC), formed at low pH 2.5 (below). The upper part demonstrates several glycoprotein fractions of bleomycin labelled with In-111 when performed at normal pH 7. BLMC consists of <10% of total BLM. At low pH, approximately 95% of In-111 will form In-111–BLMC. The labelling efficiency was >98% (< 2% free In-111). Modified from [10].

activity was 75–175 MBq, usually 75–85 MBq; the specific activity was approximately 100 MBq/mg of In-111–BLMC. The preparation procedure was performed under sterile and pyrogen-free conditions.

Patients

The patient population consisted of 28 consecutive subjects, with an active malignant disease in the head and neck region. Informed consent was obtained from each patient before injection. The histological diagnoses, locations of malignant tissue and pTNM-stagings at the time of investigation are listed in Table 1. Almost all patients were subsequently operated on, and the types of surgery are also listed in Table 1.

Gamma imaging

All patients were imaged using Siemens Rota or Picker Prism gamma camera. Patients were generally imaged three times, usually at 1 h, 4 h and 20–24 h after the injection. 5 patients were imaged more than three times. 2 patients were studied up to 5 days, but because of the long duration of the investigation, this protocol could not be applied to all patients. The matrix size was 128 × 128, and medium energy collimator for both γ-energy peaks of In-111 (173 keV and 247 keV; 20% windows) were utilised. The gamma camera was connected to a PDP 11/40 computer using Gamma-11 software. The single-photon emission computed tomography (SPECT) method was applied in 5 patients by collecting 60 45-sec frames (6° angles) at 24 h using a 64 × 64 matrix. Uptakes in gamma images were analysed using region-of-interest (ROI) technique. The target-to-non-target ratio in the neck area was calculated by taking target ROI and the same non-target ROI of the contralateral side (mirror technique). The tumour-to-background ratios (TBRs) are listed as ranges in Table 1; this range includes the variation of both time and location.

Pharmacokinetic studies

Blood and urine samples obtained up to 72 h after injection were collected from 5 patients. Urine was collected from all patients for the first 24 h. Hourly samples were taken during the first 4 h. After that the sampling interval was 4 h.

Surgical specimens

Tumour samples were obtained by routine surgical excision and further studied while fresh. Some normal tissue specimens obtained at surgery were also analysed for radioactivity. The samples were weighed, counted for radioactivity against an In-111 standard (LKB 1282 Compugamma, Wallac, Turku, Finland). For further analysis samples were first fixed in formalin and embedded in

Table 1. Results of In-111*–BLMC scintigraphy of characterised head and neck tumours*

Patient (age/sex)	Hist. Dgn.	Location	Stage (pTNM)	Surgery	Imagings (hours)	TBR	Neck US FNAC
1 (60/F)	SCC	sL	$T_1N_0M_0$	SLE	1,4,24,72	1.8–2.2	neg
2 (84/M)	AC	NC	$T_3N_0M_0$	PME	1,2,4,22	1.4–1.8	neg
3 (63/M)	SCC	Ph,NM	$T_2N_2M_0$	PPE,RND	1,3,5,20	1.0–1.4	⌀ 2.5 cm
4 (44/M)	SCC	tL,Ph	$T_4N_2M_0$	TLE,PPE,RND	1,4,24,72,120	1.2–2.8	⌀ 2.0 cm
5 (46/M)	SCC	NM,UP	$T_0N_2M_0$	RND	1,4,24	1.3–1.8	⌀ 3.0 cm
6 (55/M)	SCC	Ph	$T_2N_1M_0$	RT,NO	1,4,24	1.1–1.5	2 × ⌀ 0.6 cm
7 (76/M)	SCC	NR	$rT_2N_0M_0$	TR	1,24,72,120	1.3–2.9	⌀ 3.0 cm
8 (62/M)	SCC	NM	$T_xN_2M_0$	RND	1.4.24	1.3–1.7	5 × ⌀ 2.0 cm
9 (76/M)	SCC	To	$T_2N_0M_0$	HGE	1,4,24	1.1–1.7	⌀ 1.0 cm
10 (63/M)	SCC	OC	$T_2N_0M_0$	TR	1,4,24	1.1–1.6	neg
11 (62/M)	SCC	NM,UP	$T_0N_3M_0$	RND	1,4,24	1.6–2.8	⌀ 6.0 cm
12 (84/F)	NB	NC	$T_3N_0M_0$	TR	1,4,24	1.2–1.3	neg
13 (78/M)	SCC	tL	$T_3N_0M_0$	TLE	1,4,24	1.1–1.6	neg
14 (60/M)	SCC	L,Ph	$T_4N_0M_0$	RT,NO	1,4,24	1.1–1.9	neg
15 (73/M)	SCC	Ph	$T_1N_0M_0$	RT,NO	1,4,24	1.1–1.7	neg
16 (58/M)	SCC	tL	$T_4N_2M_0$	TLE,RND	1,4,24	1.1–1.4	2 × ⌀ 2.0 cm
17 (80/M)	FTC	NM	$T_xN_{1b}M_0$	RT,NO	1,3,24	1.1–1.6	⌀ 5.0 cm
18 (53/F)	AC	OC	$T_2N_0M_0$	TR,RND	1,4,24	1.1–1.9	neg
19 (75/M)	SCC	NM,UP	$T_{2x}N_2M_0$	RND	1,4,24	1.2–1.5	⌀ 2.0 cm
20 (65/M)	SCC	L	$T_2N_0M_0$	TLE	3,5	1.0–1.2	neg
21 (69/F)	SCC	To	$T_3N_0M_0$	RT,NO	3,5,22	1.3–1.6	nd, CT
22 (69/F)	AC	EL,NM	$T_xN_2M_0$	TR	3,5	1.3–1.5	nd, CT
23 (63/M)	SCC	sL	$T_2N_0M_0$	TLE	1,4,24	1.3–1.4	neg
24 (52/M)	SCC	NM	$T_xN_2M_0$	TR	1,4,24	1.2–1.8	⌀ 2.0 cm
25 (68/F)	SCC	L,Ph	$T_4N_0M_0$	TLE,PPE	1,4,24	1.2–1.6	neg
26 (66/F)	SCC	To	$T_2N_0M_0$	TR,RND	1,4,24	1.4–1.7	neg
27 (64/M)	SCC	L,Ph,Lu	$T_4N_2M_1$	pRT	1,4,24	1.3–1.7	2 × ⌀ 1.5 cm
28 (75/M)	SCC	L	$T_1N_0M_0$	Rt,NO	1,4,24	1.1–1.4	neg

Abbreviations: (Histological) AAC, adenomatous cancer; FTCC, follicular thyroid cancer; NB, esthesioneuroblastoma; SCC, squamous cell cancer. (Location) EL, eyelash; L, larynx; Lu, lung; NC, nasal cavity; OC, oral cavity; Ph, pharynx; To, tongue; s, supraglottic; t, transglottic; NR, neck recurrence; NM, neck metastasis; UP, unknown primary. (Therapy) HGE, hemiglossectomy; PME, partial maxillectomy; PPE, partial pharyngectomy; RND, radical neck dissection; RT, radiation therapy; SLE, supraglottic laryngectomy; TLE, total laryngectomy; TR, tumour resection; NO, not operable; p, palliative. (Others) nd, not done (only CT); TBR, tumour to background ratio; US, ultrasonography; FNAC, fine needle aspiration cytology.

paraffin, then cut into sections of 5 μm in diameter, and staining was performed by van Giesen and haematoxylin–eosin. Immunohistochemical samples were prepared in Histostix® by fast freezing using liquid nitrogen. After cutting 4 μm thick sections cold acetone was used for fixation. The samples were stained immediately or stored at −20°. The frequency of mitoses was scored on a relative scale from + to + + + as follows: (+), <1/high power field (HPF; × 400); (++), 2–5/HPF; (+ + +), >5/HPF.

Dosimetric calculations

The estimated doses are based on MIRD formalism as reported in [24] using a MIRDOSE 3 program [25]. The mean residence times were determined from the imaging data. Source organs were drawn on scintigrams to detect the time activity distribution of regions of interest (ROIs). The mean residence time was calculated as an inverse of regression of the logarithmic time-activity curves. The S-factor for an arbitrary lesion was earlier calculated with the help of phantom measurements [26].

Other radiological investigations

All patients were examined on the injection day with ultrasonography of the neck, in 6 cases also by transoesophageal US. Fine needle aspiration cytology (FNAC) was obtained from several suspicious lymph nodes of the neck region. These findings are listed in Table 1. Most patients were examined by computed tomography before surgery. Fusion imaging technique was also applied in two patients. The SPECT study performed at 24 h was overlayed on MRI (Siemens 1.0 T). The fusion was performed by six radioactive-paramagnetic markers to fix *xyz*-axes. The method is described in detail in [27].

RESULTS

Figure 1 shows the chromatograms of BLM at normal pH and BLMC, after incubating with In-111. It shows that only one major fraction will be labelled at pH 2.5, and more than 95% will be In-111–BLMC (lower part in Fig. 1).

The blood time–activity curves are presented in Fig. 2. The half-lives of In-111 activities varied from 1.5 to 3.1 h in serum, and from 1.4 to 3.7 h in urine. The maximum activity in urine was achieved in all patients within 3 h, and the average half-life in urine was 2.0 h. In all patients >95% of the activity was excreted within 24 h.

The radioactivity uptakes of 4 cases (% injected activity per gram of tissue), also analysed histologically, are presented as histograms in Fig. 3. In surgical samples (from 22 patients) the largest tumour-to-non-tumour ratios were as follows: Fat 60:1, bone 17:1, muscle 12:1, blood 11:1. In Fig. 3 tumour uptakes of 4 representative patients are presented. Tumour uptakes varied from 0.1 to 1.0×10^{-3}% ID/g tumour. In primary tumours the mean uptake was 0.47×10^{-3}% ID/g ($n = 21$; range $0.10–0.96 \times 10^{-3}$% ID/g) and metastases 0.44×10^{-3}% ID/g ($n = 12$; range $0.11–0.95 \times 10^{-3}$% ID/g). There was no statistical difference between primary tumours and metastases (two-way Student's *t*-test). The highest uptakes in normal organs were observed in lymph nodes (0.30×10^{-3}% ID/g tissue) and salivary glands (0.32×10^{-3}% ID/g tissue). Uptakes in the following organs were also measured: Blood 0.04–

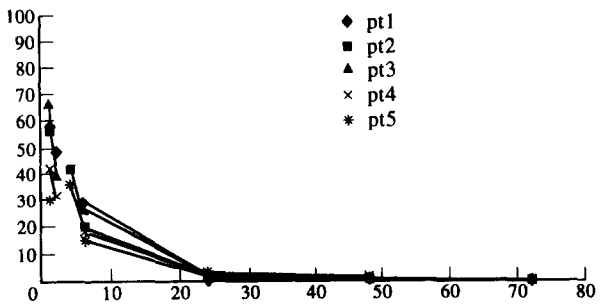

Fig. 2. Blood curves of In-111–BLMC (from 5 patients). Half-lives varied from 1.5 to 3.1 h.

0.12×10^{-3}% ID/g tissue; fat $0.01–0.05 \times 10^{-3}$% ID/g tissue; skin $0.01–0.23 \times 10^{-3}$% ID/g tissue; muscle (usually m. sternocleidomastoideus) $0.02–0.17 \times 10^{-3}$% ID/g tissue; bone (hyoid) $0.07–0.19 \times 10^{-3}$% ID/g tissue; mucous membrane $0.14–0.18 \times 10^{-3}$% ID/g tissue, and salivary gland (usually submandibular) $0.05–0.32 \times 10^{-3}$% ID/g tissue. Altogether normal tissue uptakes varied from $0.01–0.32 \times 10^{-3}$% ID/g tissue.

The imaging results are summarised in Table 1. In all patients the known primary tumour was observed. The tumour-to-background ratios varied from 1.0 to 2.9. The uptake in the image could be considered strong if this ratio was >1.20, moderate between 1.15 and 1.20, and weak or negative if the ratio was <1.15. According to this classification, strong uptakes were observed in all but 1 patient (no. 20), who had a moderate uptake. In early images (at 1–5 h) uptakes were generally low (weak or moderate). However, in 11 patients tumour uptakes were strong in all images, including early phases. In late images (after 20 h) all uptakes could be classified as strong. In 2 patients lymph nodes were observed in neck US, and were subsequently verified to be metastatic according to fine needle aspiration cytology (FNAC; patients nos 6 and 9); these were not visualised on BLMC scans. In patients with multiple lymph node involvement as confirmed by neck US and FNAC (patients nos 8, 16 and 27), the uptakes on planar images merged into each other and did not visualise separately. The TBR generally increased as a function of time, indicating a better visualisation and delineation of tumour tissue in later images, as Fig. 4 demonstrates. Uptake in upper respiratory mucosa was always observed in early images. In Fig. 4 the uptake in the nasal mucosa remained in later images and was due to a specific accumulation into the tumour in the nasal cavity.

Figure 5 demonstrates the whole body distribution of In-111–BLMC from A-P and P-A views. Rapid clearance is demonstrated by blood pool activity at early stages (at 1 h) and increasing kidney and bladder activity at early stages (at 1 h) and increasing kidney and bladder activity later (4–24 h). The same standard was used in all images to calculate uptakes in %/ID. Table 2 shows the distribution data measured at 1, 4 and 24 h. The absorbed radiation doses were calculated (MIRD-formalism) and they were: for liver 1.86×10^{-4} Gy/MBq, for kidney 7.50×10^{-4} Gy/MBq and for whole body 9.60×10^{-5} Gy/MBq, when the mean residence time was assumed to be 5 h. The tumour dose could also be calculated from the phantom measurements

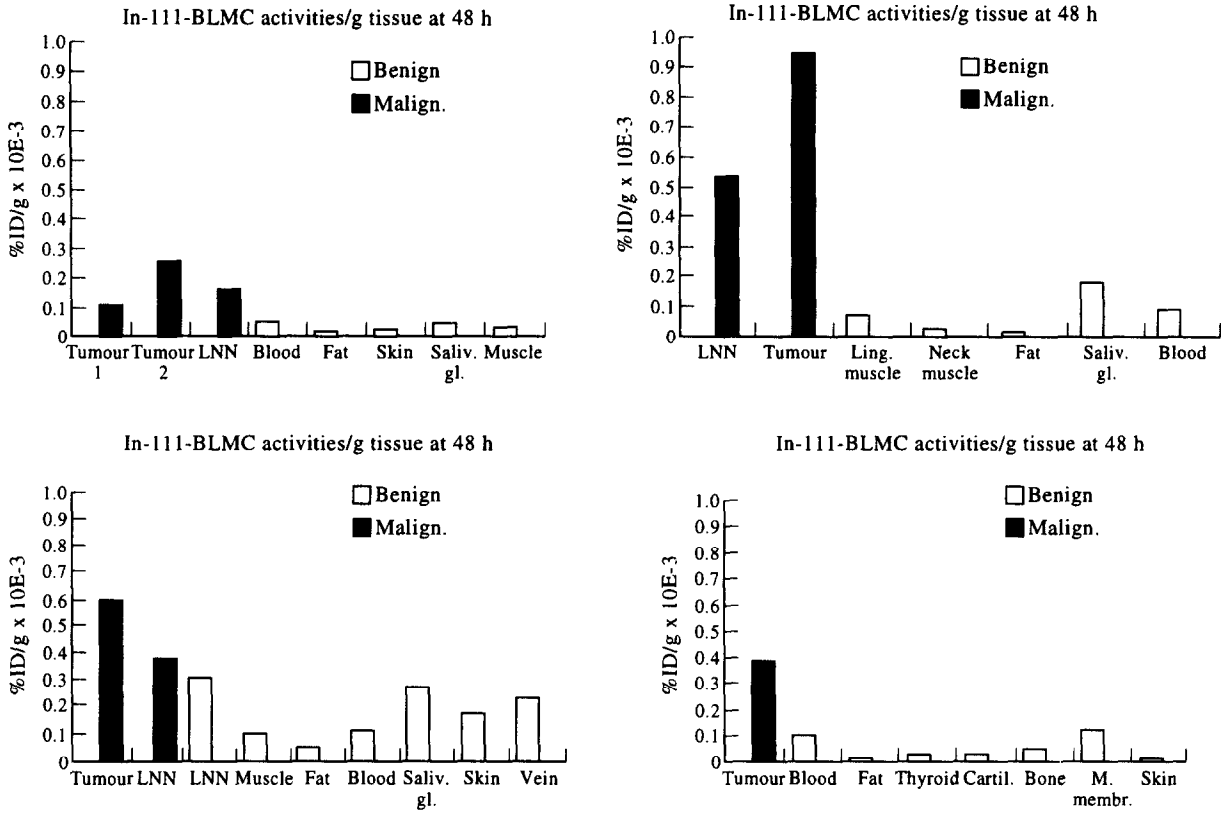

Fig. 3. In-111–BLMC activities in various surgical samples taken from 4 patients 48 h after injection. Upper panel; left: radical neck dissection for squamous cell cancer, unknown primary, 63 year old male, $T_xN_2M_0$ (patient no. 8). Upper panel; right: radical neck dissection for squamous cell cancer of the tongue, 62 year old male, $T_0N_3M_0$ (patient no. 11). Lower panel; left: radical neck dissection and total laryngectomy for squamous cell cancer of the larynx, 44 year old male, $T_4N_2M_0$ (patient no. 4). Lower panel; right: total laryngectomy for squamous cell cancer of the larynx, 78 year old male, $T_3N_0M_0$ (patient no. 13). LNN, lymph node.

[26] and we obtained 2.04×10^{-3} Gy/MBqh for tumour, which gives 1.0 Gy with injected activity of 100 MBq and mean residence time of 5 h. The highest normal organ dose was in the kidney, all other organ doses were lower. Figure 6 demonstrates a squamous cell carcinoma neck metastasis (patient no. 11) at 4 and 24 h after BLMC injection. In the last image at 24 h the uptake is almost entirely concentrated into the tumour, no basal uptake is seen. No false positive findings were observed in these patients. In Fig. 7 a rather strong uptake in a primary pharynx cancer can already be observed at 1 and 4 h. In this patient a nonspecific uptake in the shoulder joint was detected in early images (Fig. 7), but this uptake disappeared later. In one patient a lung metastasis in the right upper lobe was visualised (patient no. 27). No adverse or allergic reactions were observed in these patients. Figure 8 demonstrates a strong uptake in a squamous cell cancer of the buccal mucosa in a SPECT study 24 h after injection. The corresponding MRI slices are also shown (Fig. 8). By using this fusion imaging technique, a 3-D image of a cancer of the base of the tongue is also shown (Fig. 9). The fusion was performed by six radioactive-paramagnetic markers to fix *xyz*-axes and a SPECT study was performed 24 h after injection. In 5 patients, also studied with SPECT, the delineation of lesions was better than in planar images.

In our patient population we had the following tumour stage distribution (UICC 1987; pTNM Classification of Malignant Tumours): Stage I 3 patients; Stage II 8 patients;

Table 2. ROI analysis in head and neck tumour patients at different times after In-111*–BLMC injection. The mean uptakes in organs are presented as % of injected dose, based on serial gamma imaging*

Organ	1 h	4 h	24 h
Spleen	0.39%	0.19%	0.024%
Liver	3.80%	1.20%	0.25%
Kidney	6.70%	1.70%	0.27%
Bladder	18.40%	5.80%	0.15%
Heart	3.60%	0.82%	0.066%
Bone marrow*	1.30%	0.30%	0.023%

*Calculated from blood data according to [43]

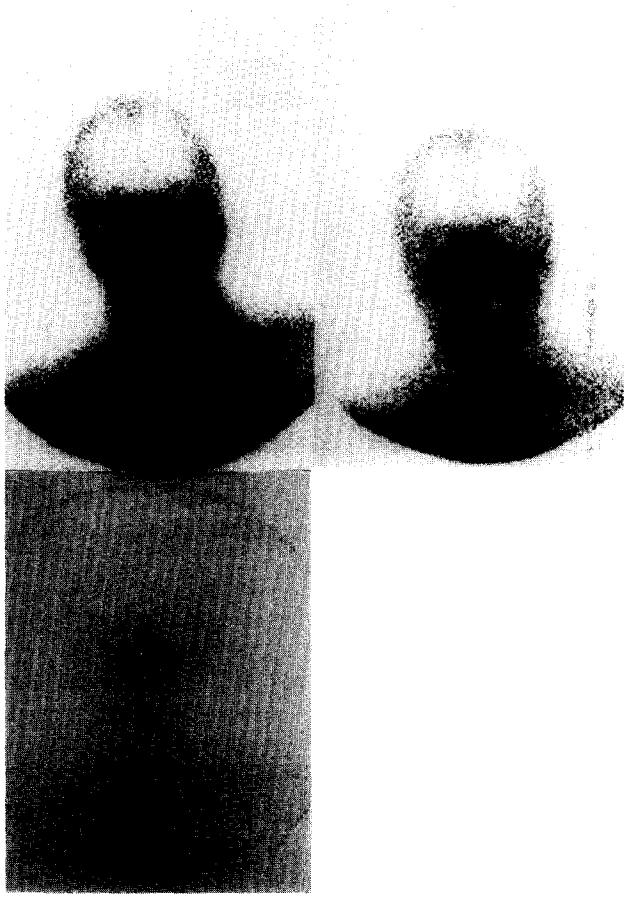

Fig. 4. Anterior planar scintigrams at 1, 4 and 22 h, from an adenomatous cancer in the nasal cavity (arrow; patient no. 2).

Stage III 4 patients; Stage IV 13 patients. In-111–BLMC imaging confirmed the staging by detecting distant metastases (patient no. 27; Table 1) and regional lymph node involvement in 11/11 patients. Tumour size could not be determined from gamma images. Table 3 represents the TBRs on In-111–BLMC scans, absolute uptakes in tissues and tumour-to-blood ratios in patients, where the grade of mitoses was calculated from histomorphological samples. Table 3 demonstrates that TBRs and absolute uptakes tend to increase with the frequency of mitoses.

DISCUSSION

In this study we have demonstrated substantial tumour targeting by using In-111–BLMC in head and neck cancer. In surgical samples, uptakes of up to 0.95×10^{-3}% ID/g tumour were observed (Fig. 3) at 48 h, the mean being approximately 0.45×10^{-3}% both in the primary tumours and metastases. Normal tissue uptakes varied from 0.01–0.32×10^{-3}% ID/g tissue, clearly below average tumour or metastasis uptakes.

In another study, the highest uptake observed at 8 h in non-small cell lung carcinoma by using Co-57-BLM was 8.85×10^{-3}% ID/cm^3 [6]. However, the results of these studies cannot be directly compared, even though the radioactivity half-life in the tumour is known in our patients, and we have an estimate of each tumour tissue density. Thus, the absolute uptake can be extrapolated to the 8-h level in our material. The main reason is that In-111–BLMC and Co-57–BLM have characteristic kinetic properties; this has also been verified in our own patients injected both with In-111–BLMC and Co-57–BLM. In late images the radioactivity was almost entirely concentrated into the tumours as Figs 5 and 7 demonstrate. In-111–BLMC apparently has very fast clearance both from urine and from blood. For therapeutical applications the excretion rate into urine must be taken into consideration. However, the dose to the urinary tract can be relieved by pharmacologically enhancing diuresis.

In this study, the overall specificity was 100% when using surgical findings as a reference. The uptakes in some larger joint areas observed in early images, as Fig. 7 demonstrates, all disappeared in later images (Fig. 4). Findings in our surgical samples did not explain the reason for this uptake. Rather high uptakes were, however, observed in some samples of oral mucosa, although not causing any false positive interpretations. We observed high uptakes in some surgically removed salivary samples although they had not been visualised on any In-111–BLMC scans. Some surgically extirpated benign lymph nodes also showed considerable uptakes. In the detection of neck metastases we obtained a sensitivity of 84.6% when using ultrasound as a reference. The detection rate of lymph nodes was correct in 17 out of 19 surgically verified metastases.

In-111–BLMC imaging was accurate in classifying all stage IV tumours, although tumour size could not be directly estimated from gamma images; the presence of neck node involvement and distant metastases could be determined and was helpful for tumour staging in each patient.

Table 3. Results of tissue analysis in head and neck tumours characterised by In-111–*BLMC injection*

Sample/ patient no.	Primary/ metastasis	Organ	Grade	Frequency of mitoses	Tumour-to-background ratio (scan)	Tumour-to-blood ratio (tissue)	
3	P	Tonsil	2	+ +	1.4	1.9	0.25
3	M	Lymph node	2	+ +	1.0	1.2	0.11
11	M	Lymph node	3	+ + +	2.8	11.0	0.95
16	P	Larynx	3	+ + +	1.4	3.1	0.64
16	M	Lymph node	3	+ + +	1.1	2.8	0.48
20	P	Larynx	1	+	1.2	1.2	0.10
22	M	Lymph node	3	+ + +	1.5	3.4	0.58
26	P	Tongue	3	+ + +	1.7	3.3	0.40
26	M	Lymph node	NA	0	1.4	1.4	0.28

P, primary; M, metastasis.

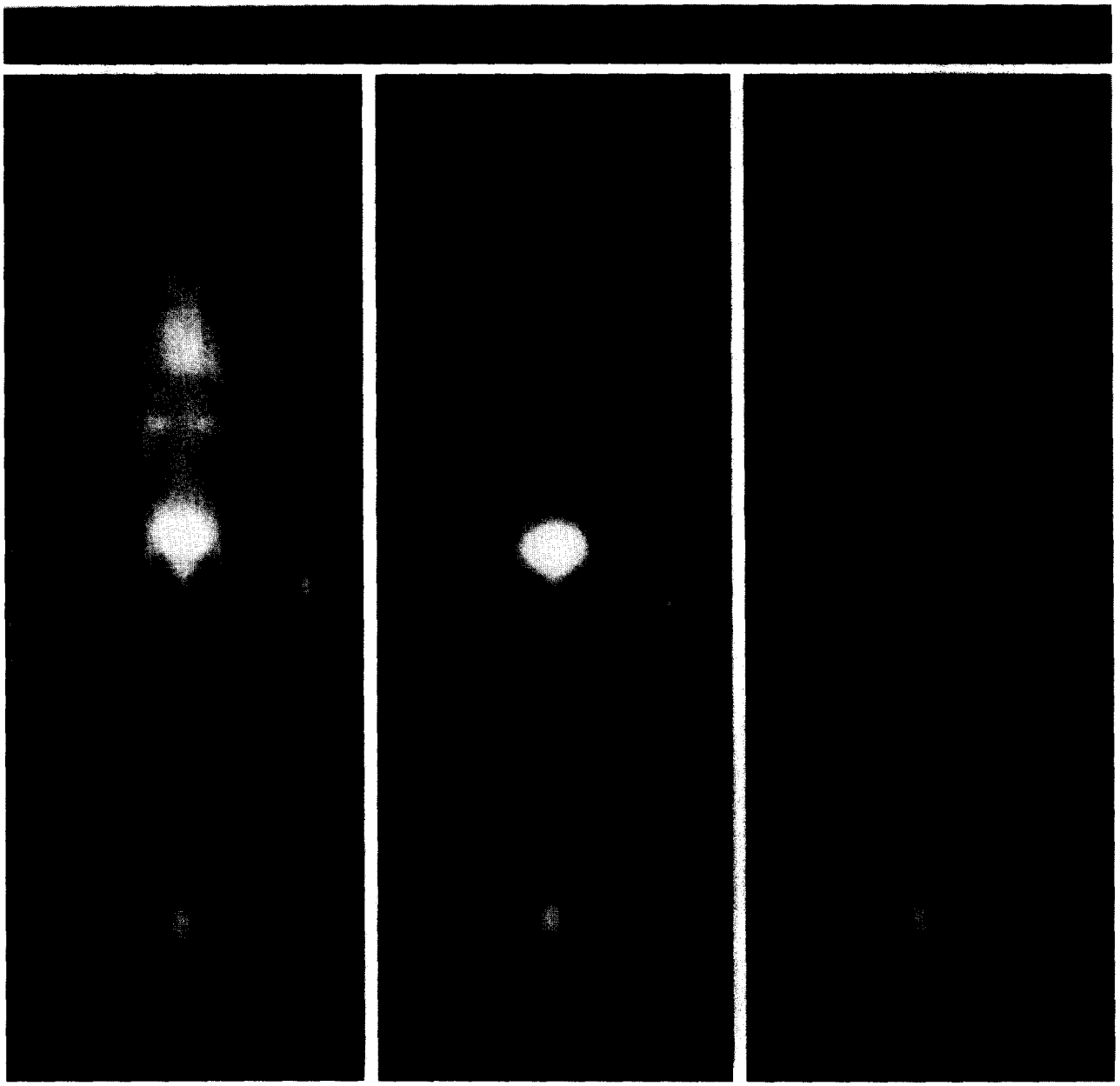

Fig. 5. Whole body scintigrams at 1, 4 and 24 h demonstrating high activities in kidneys and urinary bladder and a rapid clearance of the tracer (AP-view).

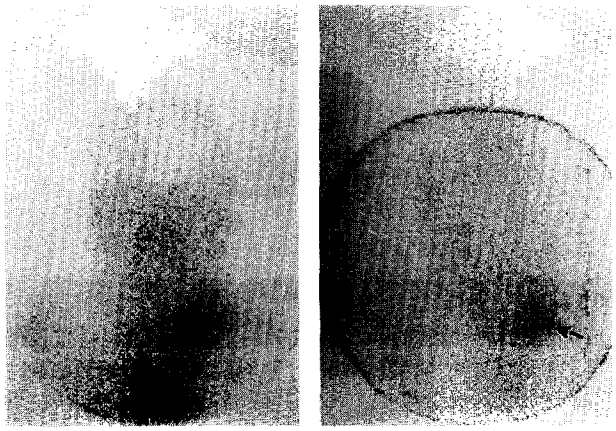

Fig. 6. Anterior planar scintigrams at 4 and 24 h of a squamous cell cancer metastasis in the neck region (arrow). No nasal uptake in late image (patient no. 11).

For accurate classification of stages I–III conventional radiological methods (CT, MRI) are required for measuring tumour dimensions. SPECT did not change the classification based on planar images, it only helped delineating small lesions better. Nevertheless, we believe that SPECT should be applied to all these patients. This was not possible in this study because of a very demanding protocol for biokinetic studies and long acquisition just prior to major operations. The limiting factor with SPECT is the long acquisition time required. Our study demonstrated a high positive predictive value (100%). Our findings are similar to those obtained for Co-57–BLM in squamous cell cancer of the thoracic region [5].

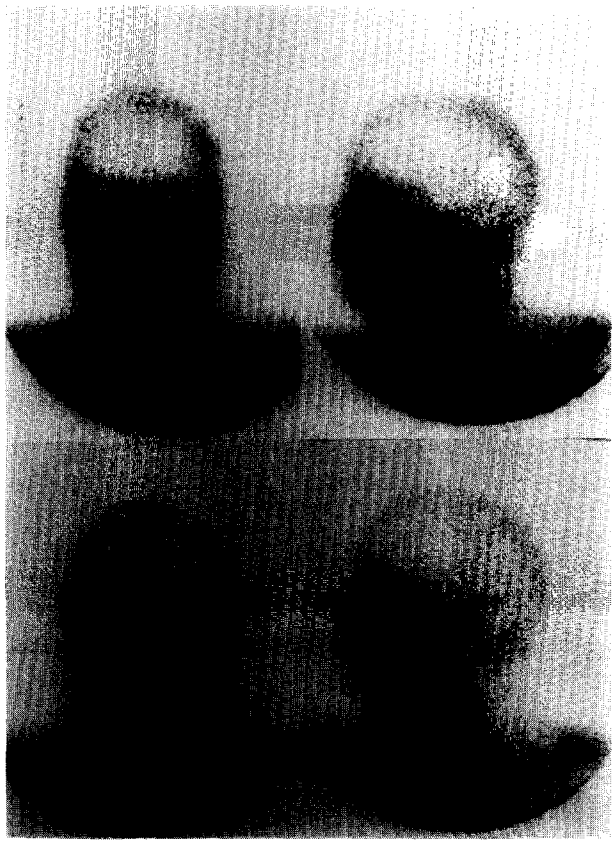

Fig. 7. Anterior planar and left lateral scintigrams at 1 and 4 h demonstrating an uptake in a primary pharyngeal cancer. Nonspecific uptakes in shoulder joints disappeared later (at 24 h) (patient no. 15).

The complex formed at low pH showed a similar chromatographical pattern, and size exclusion chromatography demonstrated similar labelling characteristics; this emphasises the fact that only the subfractions A'_{2a-c} can form the complex with In-111.

Bleomycin has clinical applications in the management of head and neck cancer in selected patient groups. It can be combined with external radiation therapy. In a study of 157 head and neck cancer patients, complete response (CR) with this combination was 80% [28], whereas CR was only 20% with radiation alone. However, large differences in disease-free and overall 5-year survival rates in favour of combined treatment were detected. In another study [29] of 104 patients, CR was 67% (combination of radiation, bleomycin and methotrexate), whereas with radiation alone it was only 45%. In a third study, bleomycin treatment combined with radiation was compared with radiation alone, and no difference was observed [30]. Even single chemotherapeutic agents, such as bleomycin, 5-fluorouracil and platinum coordination complexes, give promising therapeutic results combined with radiation. Furthermore, these treatments are better tolerated than multidrug chemotherapy programs [31]. Based on these facts, we think that selected patient groups with head and neck cancer might be treated with this bleomycin complex labelled with high activities of In-111. BLMC also forms stable compounds with other beta-emitters (i.e. Cu-64, Zn-67), which means that targeted therapy could be possible. In the chemotherapy trials 15–30 mg of bleomycin was administered [28–30] intravenously, intra-arterially or intramuscularly without side effects. We used a specific activity of 100 MBq/mg. This would correspond to 1500–3000 MBqs of In-111, which would, we believe, already be a therapeutic dose. Our estimates indicate that when injecting 3700 MBq of In-111–BLMC, and assuming a mean residence time in blood is 5 h (MIRD formalism), the total kidney dose will be 2.8 Gy (tolerance 20 Gy). The tumour dose was calculated up to 1.0 Gy in a known geometry for non-MIRD target after injecting 100 MBq [26]. If the kinetics remains constant with higher injected activities, 20 Gy will be achieved in tumours with a simultaneous kidney dose of 1.5 Gy. At this moment, however, the required tumour dose is not known. Cell survival is dependent on the physical dose, the dose rate, and the relative biological effectiveness (RBE). The biological effect of various components of radiation in radionuclide therapy is not yet fully understood and therefore tumour destruction cannot be very well predicted for the calculated data for absorbed radiation doses. In the external radiation therapy the RBE is assumed to be 1, as verified experimentally, whereas for Auger-electrons bound to DNA the RBE is in the range 7–9 [32, 33]. This local effect on the cellular level is dependent on the activity outside the cell, in the cytoplasm and within the nucleus, parameters that must be studied separately [33].

We find the positive correlation between the amount of In-111–BLMC uptake and mitotic activity interesting. This leads to the conclusion that there lies a specific mechanism beyond the tumour-seeking behaviour of this agent. Bleomycin is mainly intracellular [34, 35] and seeks the nucleus and nuclear membrane. In-111–BLMC [36] has

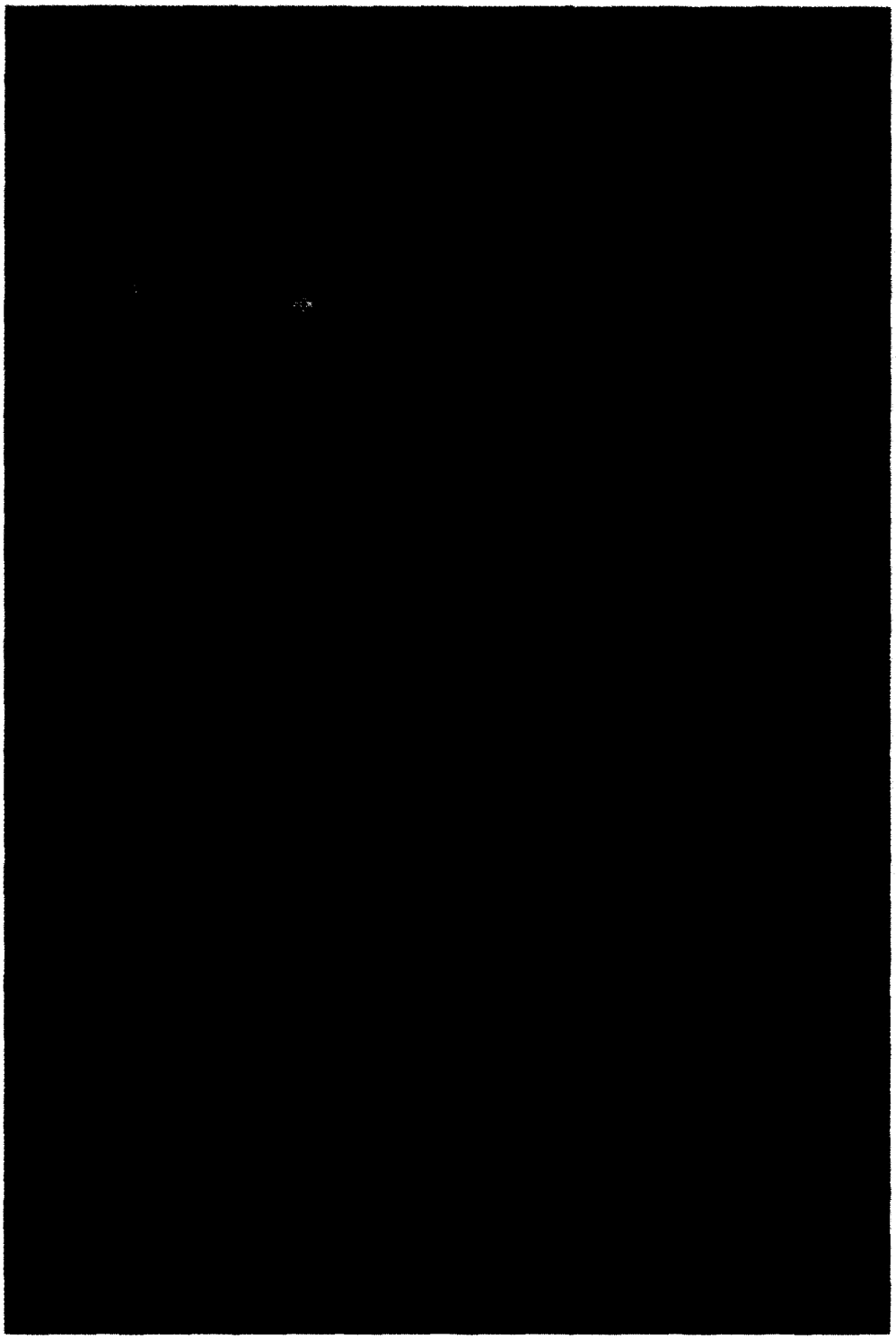

Fig. 8. SPECT study at 24 h of a squamous cell cancer of the buccal mucosa. The corresponding MRI slices are also shown.

Fig. 9. 3-D image of a cancer from the base of the tongue (outlined arrow) is shown by using a fusion imaging technique (SPECT study at 24 h on MRI (1.5 T)). The fusion was performed by six radioactive-paramagnetic markers to fix *xyz*-axes and two of these markers (solid arrows) are shown; the strongest uptake demonstrates the primary tumour (right image).

been found with great frequency (78%) in the nucleus and nuclear membrane of a small cell lung cancer line. The complex cleaves DNA strands on the cell nuclear membrane causing chromosomal aberrations, and it is known that In-111–BLMC causes more aberrations than bleomycin alone [37]. Radiolabelled BLM binds to DNA with specific mechanisms, and the cleavage sites are also known [38, 39].

Bleomycin is known to bind to guanosine–cytosine-rich portions of DNA via association of "S" tripeptide [40] in the amino terminal and also by intercalation of the bithiazole rings. The cytotoxicity is cell-cycle-phase specific for the G2 phase, even though some activity is observable in the G1 phase and no change in plateau phase versus logarithmic growth cells can be observed [41, 42]. This G2/early mitosis specificity has been thought to be the mechanism of uptake of the tumour-seeking behaviour of labelled BLMC. Recently, it was shown that the Co-57–BLM concentration, as measured *in vivo* by SPECT, correlates well with the DNA-content of the tumour [6]. Tumours with higher uptakes had a poorer response to chemotherapy. Therefore, it might be possible to recognise patients with poor response to chemotherapeutics (cyclophosphamide, doxorubicin, vincristine, etoposide and cisplatin) and offer them an alternative in the form of radiochemotherapy, e.g. by In-111–BLMC.

1. Umezawa H, Maeda K, Takeuchi K, Okami Y. New antibiotics, bleomycin A and B. *J Antibiot (A)* 1966, **19**, 200–209.
2. Umezawa H, Ishizuka M, Maeda K, Takeuchi T. Studies on bleomycin. *Cancer* 1967, **20**, 891–895.
3. Renault H, Henry R, Rapin J, Hegesippe M. Chelation de cations radiactifs par un polypeptide: la bleomycine. In: *Radiopharmaceuticals and Labelled Compounds*, Vol. II, IAEA, Vienna, 1973, 195–202.
4. Nieweg OE, Piers DA, Beekhuis H, Sluiter HJ, Wal AM van der, Woldring MG. 57Co-bleomycin scintigraphy for the staging of lung cancer. *Cancer* 1989, **63**, 1119–1122.
5. Frederiksen PB, Christensen JB, Veilstedt H, Rasmussen JW, Pedersen B, Edeling C-J. 57Co-bleomycin scintigraphy for the preoperative detection and staging of lung tumors. *Nucl Med* 1988, **27**, 79–82.
6. Even-Sapir E, Bettman L, Iosilevsky G, *et al.* SPECT quantitation of cobalt-57-bleomycin to predict treatment response and outcome of patients with lung cancer. *J Nucl Med* 1994, **35**, 1129–1133.
7. Thakur ML, Merrick MV, Gunasekera SW. Some pharmacological aspects of a new radiopharmaceutical, 111In-bleomycin. In: *Radiopharmaceuticals and Labelled Compounds*, Vol. II, IAEA, Vienna, 1973, 183–193.
8. Hou D-Y, Hoch H, Johnston GS, *et al.* A new 111-In–bleomycin complex for tumor imaging: preparation, stability, and distribution in glioma-bearing mice. *J Surg Oncol* 1984, **25**, 168–175.
9. Gment G, Matejka M, Porteder H, Sinzinger H. Indium 111-A–bleomycin—a new tracer for imaging orofacial neoplasms. *J Oral Maxillofac Surg* 1988, **46**, 742–745.
10. Hiltunen JV, Kairemo KJA, Nikula TK. Pharmacokinetic properties of low pH In-111–bleomycin complex. In: Maddalena DJ, Snowdon GM, Boniface GR, eds. *Advances in Radiopharmacology*. Proceedings of the Sixth International Symposium on Radiopharmacology, International Association of Radiopharmacology, Wollongong University Press, Australia, 1990, 136–139.
11. Kairemo KJA, Ramsay H, Hiltunen JV, *et al.* Imaging of head and neck carcinomas with low pH 111In–bleomycin complex. *Aust NZ J Med* 1990, **20**, 448.
12. Watkinson JC, Lazarus CR, Mistry R, Shaheen OH, Maisey MN, Clarke SE. Technetium-99m(V) dimercaptosuccinin acid uptake in patients with head and neck squamous carcinoma: experience in imaging. *J Nucl Med* 1989, **30**, 174–180.
13. Cummings CW, Larson SM, Dobie RA, Weymuller EA Jr, Rudd TG, Merello A. Assessment of cobalt-57 tagged bleomycin as a clinical aid in staging head and neck carcinoma. *Laryngoscope* 1981, **91**, 529–537.
14. Higashi T, Kashima I, Shimura K, *et al.* Gallium-67 scanning in the evaluation of therapy of malignant tumors of the head and neck. *J Nucl Med* 1977, **18**, 243–249.
15. Teates CD, Preston DF, Boyd CM. Gallium-67 citrate imaging in head and neck tumors: report of co-operative group. *J Nucl Med* 1980, **21**, 622–627.
16. Goode R, Goodwin D, Burget P, Nelson L. Radioisotope scanning for tumors of the head and neck—experience with indium-111 and phosphorus-32. *Arch Otolaryngol* 1973, **97**, 313–315.
17. Kairemo KJA, Hopsu EVM. Diagnosis of tumors of the parotid gland with anti-CEA immunoscintigraphy. *Am J Roentgenol* 1990, **154**, 1259–1262.

18. Kairemo KJA, Hopsu EVM. Imaging of pharyngeal and laryngeal carcinomas with indium-111-labeled monoclonal anti-CEA antibodies. *Laryngoscope* 1990, **100**, 1077–1082.
19. Baum RP, Adams S, Kiefer J, *et al.* A novel Tc-99m labeled monoclonal antibody (174 H.64) for staging head and neck cancer by immuno-SPECT. *Acta Oncol* 1993, **32**, 747–751.
20. Soo KC, Ward M, Roberts KR, *et al.* Radioimmuno-32#scintigraphy of squamous carcinomas of the head and neck. *Head Neck Surg* 1987, **9**, 349–352.
21. Van Dongen GAMS, Leverstein H, Roos JC, *et al.* Radioimmunoscintigraphy of head and neck tumors using 99mTc-labeled monoclonal antibody E48 F(ab')2. *Cancer Res* 1992, **52**, 2569–2574.
22. Schrijvers AHGJ, Quak JJ, Uyterlinde AM, *et al.* MAb U36, a novel monoclonal antibody successful in immunotargeting of squamous cell carcinoma of the head and neck. *Cancer Res* 1993, **53**, 3524–3529.
23. De Bree R, Roos JC, Quak JJ, *et al.* Clinical imaging of head and neck cancer with 99mTc-labeled monoclonal antibody E48 IgG or F(ab')2. *J Nucl Med* 1994, **35**, 775–783.
24. Snyder WS, Fisher HL Jr, Ford MR, Warner GG. Estimates of absorbed fractions for monoenergetic photo sources uniformly distributed in various organs of a heterogenous phantom: MIRD Pamphlet no. 5. *J Nucl Med* 1969, **10** (Suppl. 3), 7–52.
25. Stabin M. MIRDOSE 3, Radiation International Dose Information Center, Institute for Science and Education, USA.
26. Kairemo KJA, Ramsay HA, Paavonen T, *et al.* Dosimetric and biokinetic aspects of indium-111–bleomycin complex in head and neck cancer—implementations for radiochemotherapy. *Cancer Detect Prevent*, in press.
27. Pohjonen H, Nikkinen P, Sipila O, *et al.* Registration and display of brain SPECT and MRI using external markers. *Neuroradiology*, 1996, **38**, 108–114.
28. Shanta V, Krishnamurti S. Combined bleomycin and radiotherapy in oral cancer. *Clin Radiol* 1980, **31**, 617–620.
29. Fu KK, Phillilps T, Silverberg T, *et al.* Combined radiotherapy and chemotherapy with bleomycin and methotrexate for advanced inoperable head and neck cancer. *J Clin Oncol* 1987, **5**, 1410–1418.
30. Vermund H, Kaalhus O, Winther F, *et al.* Bleomycin and radiation therapy in squamous cell carcinoma of the upper aerodigestive tract: a phase III clinical trial. *Int J Radiat Oncol Biol Phys* 1985, **11**, 1877–1886.
31. Eisenberger M, Jacobs M. Simultaneous treatment with single-agent chemotherapy and radiation for locally advanced cancer of the head and neck. *Semin Oncol* 1992, **19** (suppl. 11), 41–46.
32. Howell RW, Narra VR, Sastry KSR, Rao DV. On the equivalent dose for Auger electron emitters. *Radiation Res* 1993, **134**, 71–78.
33. Narra VR, Sastry KSR, Goddu SM, Howell RW, Strand S-E, Roa DV. The relative biological effectiveness of 99mTc radiopharmaceuticals. *Med Phys* 1994, **21**, 1921–1926.
34. Fujimoto J. Radioautoradiographic studies on the intracellular distribution of 14C-bleomycin in mouse tumor cells. *Cancer Res* 1974, **34**, 2969–2974.
35. Dorr RT. Bleomycin pharmacology: mechanisms of action and resistance, and clinical pharmacokinetics. *Semin Oncol* 1992 (suppl 5), 3–8.
36. Hou DY, Maruyama Y. Distribution of 111In–bleomycin complex in small cell lung cancer cells by autoradiography. *J Surg Oncol* 1992, **49**, 93–97.
37. Kasai H, Naganawa H, Takita T, *et al.* Chemistry of bleomycin. XXII. Interaction of bleomycin with nucleic acids, preferential binding to guanine base and electrostatic effect of the terminal amine. *J Antibiot (A)* 1978, **31**, 1316–1320.
38. Barranco SC, Novak JK, Humphrey RM. Response of mammalian cells following treatment with bleomycin and 1,3-*bis*(2-chloroethyl)1-nitrosourea during plateau phase. *Cancer Res* 1973, **33**, 691–694.
39. Barlogie B, Drewinko B, Schumann J, *et al.* Pulse cytometric analysis of cell cycle perturbation with bleomycin *in vitro*. *Cancer Res* 1976, **36**, 1182–1187.
40. Hou DY, Maruyama Y, Drago JR. Chromosome aberrations of human small cell lung cancer induced by a new 111In–bleomycin complex. *J Surg Oncol* 1992, **51**, 236–242.
41. Kuwahara J, Sugiura Y. Sequence-specific recognition with cleavage of DNA by metallomycin: minor groove binding and possible interaction mode. *Proc Natl Acad Sci USA* 1988, **85**, 2459–2463.
42. Kakinuma J, Orii H. DNA interaction with 57Co bleomycin. *Nuklearmedizin* 1982, **21**, 232–235.
43. Sgouros G. Bone marrow dosimetry for radioimmunotherapy: theoretical considerations. *J Nucl Med* 1993, **34**, 689–694.

Acknowledgements—The authors wish to thank Hanna Pohjonen, MSc (Eng), for producing SPECT images on MRI overlays, Tapani Korppi-Tommola, Lic Phil, for helping in image processing, and Magnus Tagesson, MSc, for helping us with dosimetric calculations. The authors are also thankful to Jukka V. Hiltunen, MSc, and Tuomo K. Nikula, MSc, both from MAP Medical Technologies, Inc. for supplying the clinical grade of In-111–BLMC.